CHAPTER II

The Passage of Radiations through Matter

ALTHOUGH THIS SUBJECT is really a part of atomic physics rather than of nuclear physics, the effects of the passage of radiations through matter are of paramount importance to all nuclear experiments; in fact, a thorough knowledge of these effects is absolutely indispensable to the experimental nuclear physicist. Many arguments treated in this chapter are primarily applications of electromagnetism; for these (Ja 62) is an excellent reference.

2-1 Introduction

There are three main types of radiation: charged heavy particles of mass comparable with the nuclear mass, electrons, and electromagnetic radiation. For all of them the interactions to be considered are electromagnetic. (Neutrons behave quite differently and will be treated in Chap. 12.) The behavior of mesons and other particles is intermediate between that of electrons and of nuclei, as will be seen from what follows.

A striking difference in the absorption of the three types of radiation is that only heavy charged particles have a range. That is, a monoenergetic beam of heavy charged particles, in traversing a certain amount of matter, will lose energy without changing the number of particles in the beam. Ultimately they will all be stopped after having crossed practically the same thickness of absorber. This minimum amount of absorber that stops a particle is its range: e.g., the range of polonium alpha particles, of energy 5.30 MeV, is 3.84 cm of air at STP (15°C and 760 mm pressure). For electromagnetic radiation, on the other hand, the absorption is exponential. Energy is removed from the beam and degraded; i.e., the intensity decreases in such a way that

$$-\frac{dI}{I} = \mu\, dx \qquad \text{(2-1.1)}$$

where I is the intensity of the primary radiation, μ is the absorption coefficient, and dx is the thickness traversed. Electrons exhibit a more complicated behavior. They radiate electromagnetic energy easily because they have a large value of e/m and hence are subject to violent accelerations

CHAPTER 2

The Passage of Radiations through Matter

under the action of electric forces. Moreover, they undergo scattering to such an extent that they follow irregular trajectories.

We shall now define a few terms which recur frequently in this chapter. Consider a parallel beam of monoenergetic particles (e.g., protons) moving through an absorber. As they travel, they lose energy. The energy lost per unit path length is the *specific energy loss* and its average value is the *stopping power* of the absorbing substance. The *specific ionization* is the number of ion pairs produced per unit path length. The specific energy loss and the specific ionization are subject to fluctuations; hence we define a mean specific energy loss, a mean specific ionization, etc. The fluctuations in energy loss also produce fluctuations in range (*straggling*). A plot of the number of particles in the beam penetrating to a certain depth gives the curve of Fig. 2-1. The abscissa R_0 of the point passed by half the particles is called the *mean range*. The abscissa R_1, the intersection of the x axis with the tangent at the point of steepest descent, is called the extrapolated range. The difference between the extrapolated and mean range is sometimes called the *straggling parameter*.

The curve showing the specific ionization as a function of the residual range is known as a *Bragg curve*. It is necessary to distinguish between the Bragg curve of an individual particle (Fig. 2-2) and the average Bragg curve for a beam of particles (Fig. 2-3).

Often the thickness is measured in g cm^{-2} of absorber. One then speaks of a mass absorption coefficient, mass stopping power, etc. The relation between the absorption coefficient μ and the mass absorption coefficient μ' is found by noting that the thickness x (in cm) is related to the thickness t (in g cm^{-2}) by

$$\rho x = t \tag{2-1.2}$$

where ρ is the density of the medium. Consequently,

$$\mu x = \frac{\mu t}{\rho} = \mu' t \tag{2-1.3}$$

and hence the mass absorption coefficient is

$$\mu' = \frac{\mu}{\rho} \tag{2-1.4}$$

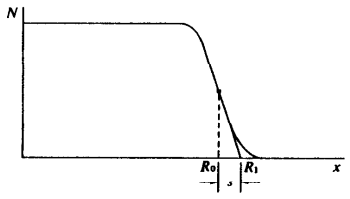

Figure 2-1 Range curve showing the number of particles in a beam penetrating to a given depth.

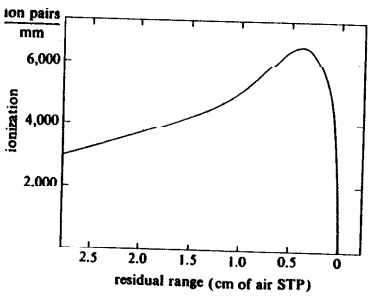

Figure 2-2 Bragg curve of an individual alpha particle. Ionization of an alpha particle, in ion pairs per millimeter, as a function of its residual range, according to experiments by Holloway and Livingston. [*Phys. Rev.*, **54**, 29 (1938).] In experiment ρ_{air} = 1.184 mg cm^{-3} (15°C, 760 mm Hg).

The atomic absorption coefficient μ_a is sometimes employed when thicknesses are measured in atoms per square centimeter; we have then, by an argument similar to the previous one,

$$\mu_a = \frac{\mu}{N} \tag{2-1.5}$$

where N is the number of atoms per cubic centimeter.

2-2 Rutherford Scattering

Consider a particle of charge ze traversing matter of atomic number Z, for instance, a proton traversing a piece of aluminum. Occasionally the proton will collide elastically with an aluminum nucleus and will undergo "Rutherford scattering"; i.e., the electrostatic repulsion from the nucleus will deflect it.

Elastic nuclear collisions give rise to large changes in the direction of the impinging particle but not, on the average, to significant energy losses. In a cloud-chamber picture (Fig. 2-4) a nuclear collision is easily

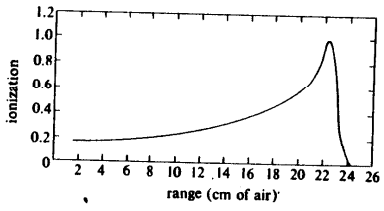

Figure 2-3 Bragg curve for a beam of protons. In experiment ρ_{air} = 1.166 mg cm^{-3}. Ordinate scale arbitrary. [R. R. Wilson, Cornell University.]

CHAPTER 2

The Passage of Radiations through Matter

distinguishable. In addition there are collisions with the extranuclear electrons. These constitute the main cause of energy loss at energies below several hundred MeV, although they produce only an extremely small scattering of heavy particles. Inelastic nuclear collisions are treated in Chap. 11.

The effect of a nuclear collision can be calculated classically as follows: Assume that the scattering center has an infinite mass (in other words, is fixed) and that it exerts a repulsive electrostatic force on the impinging proton, given by Ze^2/r^2. This force, which has a potential

$$V(r) = +\frac{Ze^2}{r} \tag{2-2.1}$$

produces a motion whose orbit lies in the plane of the fixed center and the initial velocity vector. If $\mathbf{r}$ is the radius vector from the force center (located at the origin) to the proton and $\mathbf{p} = m\dot{\mathbf{r}}$, the proton's momentum, Newton's second law of motion gives

$$\dot{\mathbf{p}} = \frac{Ze^2\mathbf{r}}{r^3} \tag{2-2.2}$$

Multiplying both sides vectorially by $\mathbf{r}$, we have

$$\mathbf{r} \times \dot{\mathbf{p}} = 0 \tag{2-2.3}$$

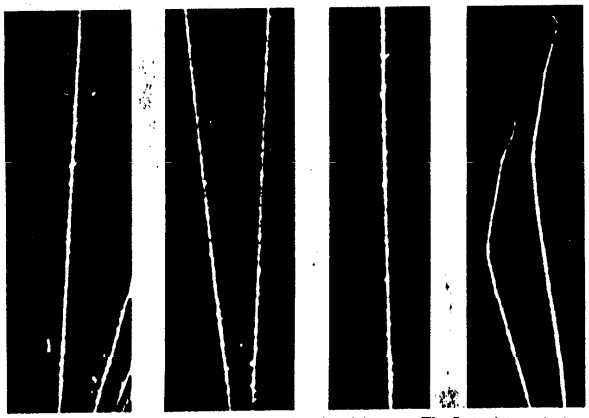

Figure 2-4 Cloud-chamber tracks of alpha rays showing delta rays. The first picture is in air, the last three in helium; the gas pressure in the chamber is such that the tracks cross about 10^{-5} g cm^{-2} of air equivalent. Note nuclear collisions in the section on the right. [T. Alper, *Z. Physik*, **67**, 172 (1932).]

Thus angular momentum

$$\mathbf{L} = \mathbf{r} \times \mathbf{p} \tag{2-2.4}$$

is a constant of the motion, since its time derivative is zero.

SECTION 2-2

Rutherford Scattering

The total energy

$$\frac{p^2}{2m} + \frac{Ze^2}{r} = E \tag{2-2.5}$$

is another constant of the motion.

The vector

$$\boldsymbol{\epsilon} = \frac{-1}{Ze^2m}\mathbf{L} \times \mathbf{p} + \frac{\mathbf{r}}{r} \tag{2-2.6}$$

which in the plane of the motion, is also constant in time, as can be verified by calculating $\dot{\boldsymbol{\epsilon}}$ according to Eqs. (2-2.1), (2-2.2), and the formula for the vector triple product.

Scalar multiplication of Eq. (2-2.6) on both sides by $\mathbf{r}$, by using the formula for the mixed triple product, gives

$$\boldsymbol{\epsilon} \cdot \mathbf{r} = \frac{L^2}{me^2Z} + r \tag{2-2.7}$$

This equation can be interpreted easily by using polar coordinates with polar axis in the direction of $\boldsymbol{\epsilon}$. Equation (2-2.7) then reads

$$\epsilon r \cos\varphi = \frac{+L^2}{me^2Z} + r \tag{2-2.8}$$

or

$$r = \frac{+L^2/me^2Z}{1 - \epsilon\cos\varphi}$$

which for $\epsilon > 1$ is the equation of a hyperbola of eccentricity ϵ.

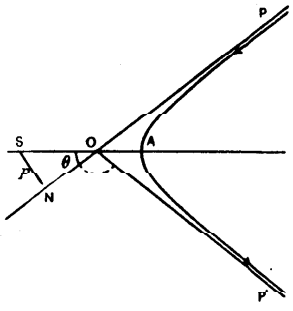

Figure 2-5 Orbit of a particle undergoing Rutherford scattering. [Original from Rutherford, *Phil. Mag.*, **21**, 672 (1911).] The notation used here is somewhat different.

The angle between the asymptotes not containing the hyperbola (Fig. 2-5) defines the deflection of the particle θ. It is found by determining the difference between the values of $\varphi = \pm\varphi_1$ for which the denominator is zero and taking the supplementary angle to this difference. One finds

$$\cos\varphi_1 = \frac{1}{\epsilon} = \sin\frac{\theta}{2} \tag{2-2.9}$$

or

$$\frac{Ze^2}{2Eb} = \tan\frac{\theta}{2} \tag{2-2.10}$$

where $b = L/(2mE)^{1/2}$ is the impact parameter, defined as the distance between the center of force and the limiting line of flight of the particle, for large values of r.

We can now calculate the probability of a deflection θ for protons crossing a foil of a substance of atomic number Z. We assume that the deflection is the consequence of a single nuclear collision. This is the case for large deflections. Small deflections are generally the result of the combined action of many collisions as will be seen later. We shall thus evaluate the nuclear-scattering cross section $d\sigma/d\omega$ and the probability of scattering through an angle between θ and $\theta + d\theta$ in crossing a foil of thickness x of a material containing N nuclei per unit volume. The probability $P(\theta)\,d\omega$ for scattering through angle θ into an element of solid angle $d\omega$ is given by

$$P(\theta)\,d\omega = \frac{d\sigma}{d\omega}Nx\,d\omega \tag{2-2.11}$$

Consider one nucleus of the scatterer and an incident beam containing one proton per unit surface area. If a proton has an impact parameter b with respect to the scatterer, the deflection is given by (2-2.10).

The number of protons dn having an impact parameter between b and $b + db$ is $2\pi b\,db = dn$, where, from Eq. (2-2.10),

$$db = -\frac{Ze^2}{4E}\frac{d\theta}{\sin^2(\theta/2)} \tag{2-2.12}$$

Hence

$$|dn| = \pi\left(\frac{Ze^2}{2E}\right)^2\frac{\cos(\theta/2)}{\sin^3(\theta/2)}\,|d\theta| \tag{2-2.13}$$

This is the number of particles deflected through an angle between θ and $\theta + d\theta$. They pass with uniform density between two cones of aperture θ and $\theta + d\theta$. The solid angle included between these cones is

$$d\omega = 2\pi\sin\theta\,d\theta \tag{2-2.14}$$

and

$$\frac{dn}{d\omega} = \frac{1}{4}\left(\frac{Ze^2}{2E}\right)^2\frac{1}{\sin^4(\theta/2)} \tag{2-2.15}$$

The quantity $dn/d\omega$ is dimensionally an area, and comparison with Eq. (2-2.11) shows that the differential-scattering cross section is

$$\frac{d\sigma}{d\omega} = \frac{1}{4}\left(\frac{e^2Z}{mv^2}\right)^2\frac{1}{\sin^4(\theta/2)} \tag{2-2.16}$$

This is the famous Rutherford scattering formula (Rutherford, 1912). Put in convenient numerical form it is

$$\frac{d\sigma}{d\theta} = 2\pi\sin\theta\,\frac{d\sigma}{d\omega} = \frac{0.8139Z^2}{E^2\,(\text{MeV})}\frac{\sin\theta}{\sin^4(\theta/2)} \times 10^{-26}\ \text{cm}^2\ \text{per nucleus} \tag{2-2.17}$$

The experimental verification was carried out in detail by Rutherford, Geiger, Marsden, and others and led to the formulation of the planetary model of the atom.

Formula (2-2.16) can be extended to other particles besides the proton by replacing Z with Zz, where z is the atomic number of the projectile. Equation (2-2.16) is not relativistic and refers to a fixed center. Moreover, it considers only Coulomb forces, neglects both the finite size of the nucleus and specific nuclear forces, and is calculated classically without regard to quantum mechanics. In spite of all these approximations, the equation gives excellent results in many practical cases, notably for the scattering of particles having a computed minimum distance of approach to a target larger than approximately $1.2 \times 10^{-13}A^{1/3}$ cm, where A is the mass number of the target. The failure of Eq. (2-2.16) for cases where this distance becomes smaller is evidence that specific nuclear forces become operative. In fact, it was just such failure that provided the first indication of the "nuclear radius."

It is possible to generalize Eq. (2-2.16) to take into account the finite mass of the target. One obtains

$$\frac{d\sigma}{d\omega} = \left(\frac{e^2zZ}{mv^2}\right)^2\frac{1}{\sin^4\theta}\frac{(\cos\theta \pm [1 - (m/M)^2\sin^2\theta]^{1/2})^2}{[1 - (m/M)^2\sin^2\theta]^{1/2}} \tag{2-2.18}$$

where M is the mass of the target and m is the mass of the projectile. For $m < M$ the positive sign only should be used before the square root. For $m > M$ the expression should be calculated for positive and negative signs and the results added to obtain $d\sigma/d\omega$. The angle θ is the laboratory angle. If the colliding particles are identical, important quantum-mechanical corrections are necessary, and Eq. (2-2.18) is no longer applicable (Mott, 1930) (see Chap. 10).

An important limiting case of Eq. (2-2.16), also valid relativistically, is obtained when the deflection angle θ is small compared with 1 rad,

$$\frac{d\sigma}{d\omega} = \left(\frac{2Zze^2}{p\beta c}\right)^2\frac{1}{\theta^4} \qquad \beta = \frac{v}{c} \tag{2-2.19}$$

For extremely small angles, which correspond to large impact parameters, the nuclear charge is screened by the atomic electrons, and Eq. (2-2.19) is invalid. It is this screening effect that prevents the equation from diverging for $\theta \to 0$. An important practical application of

Eq. (2-2.19), to the problem of multiple scattering, will be discussed later.

The Rutherford scattering formula can be obtained also by means of quantum mechanics; in this case Born's approximation (see Appendix B) happens to give the correct result. The simple derivation is given here as an example of the application of Born's approximation. The fundamental formula (see Appendix B) is

$$\frac{d\sigma}{d\omega} = \frac{1}{4\pi^2\hbar^4}\frac{p^2}{v^2}|U_{\mathbf{p}-\mathbf{p}'}|^2 \tag{2-2.20}$$

Use of Eq. (2-2.20) requires the calculation of the matrix element $U_{\mathbf{p}-\mathbf{p}'}$ for the potential Ze^2/r. We have

$$U_{\mathbf{p}-\mathbf{p}'} = Ze^2\int \frac{\exp(i/\hbar)(\mathbf{p}-\mathbf{p}')\cdot\mathbf{r}}{r}\,d\tau \tag{2-2.21}$$

This integral is best calculated by transforming it to polar coordinates with a polar axis in the direction $\mathbf{p}-\mathbf{p}'$. Designate by θ the scattering angle and by μ the cosine of the angle between $\mathbf{r}$ and $\mathbf{p}-\mathbf{p}'$, and observe that $|\mathbf{p}| = |\mathbf{p}'|$ and $|\mathbf{p}-\mathbf{p}'| = 2p\sin(\theta/2) = k\hbar$. In the integral (2-2.21) the volume element becomes $2\pi\,d\mu r^2\,dr$, and we have

$$U_{\mathbf{p}-\mathbf{p}'} = Ze^2\int_{-1}^{1}\int_0^\infty \frac{e^{ik\mu r}}{r}\,2\pi\,d\mu\,r^2\,dr \tag{2-2.22}$$

Integrating with respect to μ gives

$$U_{\mathbf{p}-\mathbf{p}'} = Ze^2 4\pi\int_0^\infty \frac{\sin kr}{kr^2}\,r^2\,dr \tag{2-2.23}$$

This last integral oscillates in value when the upper limit is considered, but it is easy to prove, for instance, by replacing Ze^2/r by $(Ze^2/r)e^{-\alpha r}$ and after integration going to the limit $\alpha \to 0$ that we must take 0 as the value at the upper limit. We thus obtain

$$U_{\mathbf{p}-\mathbf{p}'} = \frac{4\pi Ze^2}{k^2} = \frac{\pi\hbar^2 Ze^2}{p^2\sin^2(\theta/2)} \tag{2-2.24}$$

and by using Eq. (2-2.20) we find

$$\frac{d\sigma}{d\omega} = \frac{1}{4\pi^2\hbar^4}\frac{p^2}{v^2}\frac{\pi^2\hbar^4Z^2e^4}{p^4\sin^4(\theta/2)} = \frac{Z^2e^4}{4p^2v^2}\frac{1}{\sin^4(\theta/2)} \tag{2-2.25}$$

which is identical to Eq. (2-2.16).

2-3 Energy Loss Due to Ionization

In addition to the nuclear collisions mentioned above, a heavy charged particle moving through matter collides also with atomic electrons. The greatest part of the energy loss occurs in these collisions. Sometimes the atomic electrons receive so much energy that they become free and are clearly visible in cloud-chamber pictures (Fig. 2-4, delta rays). Sometimes the atom is excited but not ionized. In any case, the energy for these processes comes from the kinetic energy of the incident particle, which is thereby slowed down. Figure 2-5 gives a plot of specific ionization versus range. Since the energy spent in forming an ion pair in a gas happens to be approximately independent of the energy of the particle forming the ions, this curve approximates the curve of specific energy loss.

To calculate the rate of energy loss by a particle of charge ze as it progresses through a medium containing $\mathcal{N}$ electrons cm^{-3}, we first consider the electrons as free and at rest. The force between the heavy particle and the electron is ze^2/r^2, where r is the distance between them. The trajectory of the heavy particle is not appreciably affected by the light electron, and we can consider the collision as lasting such a short time that the electron acquires an impulse without changing its position during the collision. By this hypothesis the impulse acquired by the electron must be perpendicular to the trajectory of the heavy particle and can be calculated by

$$\Delta p_\perp = \int_{-\infty}^{\infty} e\mathscr{E}_\perp\,dt = \int e\mathscr{E}_\perp\frac{dx}{v} = ze^2\int_{-\infty}^{\infty}\frac{1}{r^2}\cos\theta\,\frac{dx}{v} \tag{2-3.1}$$

where $\mathscr{E}_\perp$ is the component of the electric field at the position of the electron normal to the trajectory of the particle (Fig. 2-6) and v is the velocity of the heavy particle, which is taken to be constant during the collision. The integral is easily evaluated by applying Gauss's theorem to a cylinder of radius b having the trajectory as its axis. Note that the flux of $\mathscr{E}$ through this cylinder is given by

$$\phi = \int \mathscr{E}_\perp\,2\pi b\,dx = 4\pi ze \tag{2-3.2}$$

Replacing the second integral of Eq. (2-3.1) by its value obtained from Eq. (2-3.2),

$$\Delta p = \frac{2ze^2}{bv} \tag{2-3.3}$$

The energy transferred to the electron is then

$$\frac{(\Delta p)^2}{2m} = \frac{2}{m}\left(\frac{ze^2}{bv}\right)^2 \tag{2-3.4}$$

and since there are $2\pi\mathcal{N}b\,db\,dx$ electrons per length dx that have a

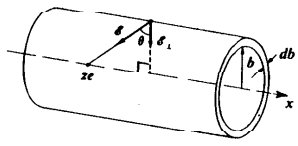

Figure 2-6 Transfer of momentum to an electron by a moving heavy charge.

distance between b and $b + db$ from the heavy ion, the energy loss per path length dx is

$$\frac{dE}{dx} = 2\pi N \int b\,db \frac{(\Delta p)^2}{2m} = 4\pi N \frac{z^2e^4}{mv^2} \int_{b_{min}}^{b_{max}} \frac{db}{b}$$

$$= 4\pi N \frac{z^2e^4}{mv^2} \log \frac{b_{max}}{b_{min}} \qquad (2\text{-}3.5)$$

This is the stopping power of the absorbing medium. At first, one might be tempted to extend the integral from zero to infinity, obtaining a divergent result. To do so, however, would be incompatible with the hypotheses under which Eq. (2-3.4) was derived; for instance, distant collisions last a long time, and the corresponding energy transfer is not given by this equation.

Equation (2-3.5) also shows that the energy loss due to collisions with nuclei is negligible compared with the energy loss to electrons. In considering nuclear collisions we would find a factor Z^2 in the numerator and also the nuclear mass instead of the electron mass in the denominator. The increase in the denominator is the dominating factor.

We shall now discuss the values of b_{max} and b_{min} which are suitable to the problem. For b_{max} we consider that the electrons are not free but are bound in atomic orbits. The adiabatic principle of quantum mechanics states that one cannot induce transitions from one quantum state to another by a time-dependent perturbation if the variation of the perturbation is small during the periods τ of the system. In our case it can be assumed that the duration of the perturbation is the time b/v during which the heavy particle is near the electron and that in order to produce transitions the condition $b/v < \tau = 1/\nu$ must be fulfilled. This determines b_{max} as $< v/\langle\nu\rangle$, where $\langle\nu\rangle$ is an appropriate average of the frequencies of the atom. Taking relativistic corrections into account, the duration of the perturbation is shortened by a factor $(1 - \beta^2)^{-1/2}$. The limit for b_{max} given by the adiabatic condition then becomes

$$b_{max} = \frac{v}{\langle\nu\rangle(1 - \beta^2)^{1/2}} \qquad (2\text{-}3.6)$$

The limits for b_{min} are several: first, in an electric collision it is impossible to change the momentum of an electron by an amount greater than $2mv$ as can be easily seen if we consider the heavy particle at rest and the electron impinging on it. This implies, according to Eq. (2-3.3), a minimum classical impact parameter

$$b_{min\ cl} = \frac{ze^2}{mv^2} > \frac{Ze^2}{mc^2} = Zr_0 \qquad (2\text{-}3.7)$$

where r_0 is the classical radius of the electron, 2.8×10^{-13}cm.

Quantum mechanics gives another limit to b_{min} inasmuch as the electron can be localized with respect to the heavy ion only to the

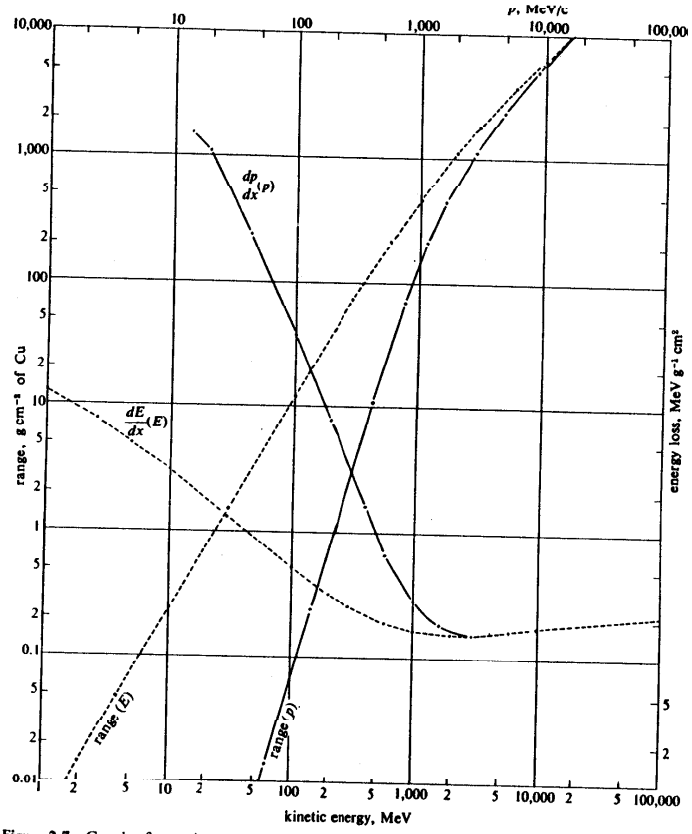

Figure 2-7 Graph of stopping power vs. energy and of specific momentum loss versus momentum for heavy particles in copper. In the same figure range-energy and range-momentum relations for protons in copper. All scales are logarithmic. The figure may be used for other particles. Remember $-dE/dx = z^2\lambda(v)$ and the scaling laws of Sec. 2-3.

accuracy of its de Broglie wavelength; that is,

$$b_{\min\,qm} > \frac{\hbar}{p} = \frac{\hbar(1-\beta^2)^{1/2}}{mv} \tag{2-3.8}$$

We must now introduce in Eq. (2-3.5) the smallest value of $b_{\max}$ and the largest value of $b_{\min}$. Over a large velocity interval this gives

$$-\frac{dE}{dx} = \frac{4\pi z^2 e^4}{mv^2}\mathcal{N}\log\frac{mv^2}{\pi\hbar\langle\nu\rangle(1-\beta^2)} \tag{2-3.9}$$

The quantity $2\pi\hbar\langle\nu\rangle$ is a special average of the excitation and ionization potentials in the atom of the stopping material. It can be calculated by using the Thomas–Fermi model of the atom. Bloch (1933) found that it is approximately proportional to Z,

$$2\pi\hbar\langle\nu\rangle = I = BZ \tag{2-3.10}$$

A better semiempirical formula is $I/Z = 9.1(1 + 1.9Z^{-2/3})$ eV for $B \geq 4$. A more precise calculation of the stopping power, performed by Bethe, gives

$$-\frac{dE}{dx} = \frac{4\pi z^2 e^4}{mv^2}\mathcal{N}\left[\log\frac{2mv^2}{I(1-\beta^2)} - \beta^2\right] \tag{2-3.11}$$

A sample of the stopping-power curve is given in Fig. 2-7.

At very low velocities, i.e., when v is comparable with the velocity of the atomic electrons around the heavy particle (in the case of hydrogen, $v = c/137$), the heavy ion neutralizes itself by capturing electrons for part of the time. This result is a rapid falloff of ionization at the very end of the range. On the other hand, at extremely high energies, with $v \sim c$, ionization increases, for several reasons. The relativistic contraction of the Coulomb field of the ion increases $b_{\max}$ according to Eq. (2-3.6) and decreases $b_{\min}$ according to Eq. (2-3.8). Part of the energy is carried away as light (Cerenkov radiation). This last effect will be discussed in Sec. 2-5.

The general form of Eq. (2-3.11) allows us to draw some conclusions of considerable practical importance. We can write Eq. (2-3.11) as

$$-\frac{dE}{dx} = z^2\lambda(v)$$

or remembering that the kinetic energy of a particle of mass M is $E = M\epsilon(v)$, where ϵ is a function of the velocity only, we have, using E as a variable,

$$-\frac{dE}{dx}(E) = z^2\lambda_E(E/M) \tag{2-3.12}$$

or, using v as a variable,

$$-\frac{dv}{dx}(v) = \frac{z^2}{M}\lambda_v(v) \tag{2-3.13}$$

Relations (2-3.12) and (2-3.13) allow us to write the energy loss as a function of energy for any particle, once the energy loss as a function of energy is known for protons. In particular, protons, deuterons, and tritons of the same velocity have the same specific energy loss.

Similar scaling relations obtain for the range. Using the velocity as a variable, one has

$$K_v(v) = \int_0^v \left(\frac{dv}{dx}\right)^{-1} dv = \frac{M}{z^2}\int_0^v [\lambda_v(v)]^{-1}\,dv = \frac{M}{z^2}\rho_v(v) \tag{2-3.14}$$

or, using energy as a variable,

$$R_E(E/M) = \frac{M}{z^2}\rho_E(E/M) \tag{2-3.15}$$

For clarity we have indicated explicitly the independent variable to be used in the functions.

Equation (2-3.14) is not exact, for the neutralization phenomena occurring at the end of the range and other corrections are neglected; but it is sufficiently accurate for most cases, excluding very low energies. As an example of the application of Eq. (2-3.15) we can verify that a deuteron of energy E has twice the range of a proton of energy $E/2$.

A semiempirical power law valid from a few MeV to 200 MeV for the proton range-energy relations is

$$R(E) = \left(\frac{E}{9.3}\right)^{1.8}$$

where E is in MeV and R is in meters of air.

Sample numerical data on range-energy relations are provided in Fig. 2-7 and in Fig. 2-8, which presents a nomogram useful for approximate estimates.

The mass stopping power is more often used than $-dE/dx$, the (linear) stopping power. The mass stopping power depends on the factors $\mathcal{N}/\rho$ and I of the stopping substances. The number of electrons per cubic centimeter, $\mathcal{N}$, is roughly proportional to the density ρ. If this proportionality were exact, only the dependence of I on Z would influence the mass stopping power. Actually, $\mathcal{N}/\rho$, and hence the mass stopping power, decreases with Z.

Heavier ions, such as C^{12}, O^{16}, and A^{40}, are slowed down by ionization loss in much the same way as alpha particles. The part of the range where the effective charge on the ion changes is emphasized, and the maximum stopping power is reached at velocities increasing with Z. For example, for C^{12} and A^{40} the maximum specific ionization occurs at approximately $v/c = 0.037$ and 0.059, which correspond to energies of 8 and 65 MeV, respectively. At lower energies the decrease of the effective nuclear charge overcompensates the effect of the diminishing velocity and the stopping-power decrease with energy. In other words, the behavior is the same, on an exaggerated scale, as that observed at the end of the Bragg curve for protons and alpha particles (Fig. 2-2).

The extreme case is furnished by fission fragments. Their effective

charge is large, reaching about $20e$ at the beginning of the range; and nuclear collisions are an important source of energy loss. If a fragment of atomic number Z_1 crosses a medium of atomic number Z_2 and nuclear mass M_2, the specific energy loss to nuclei is proportional to

$$Z_1^2 \frac{Z_2^2}{M_2} \qquad \text{(2-3.16)}$$

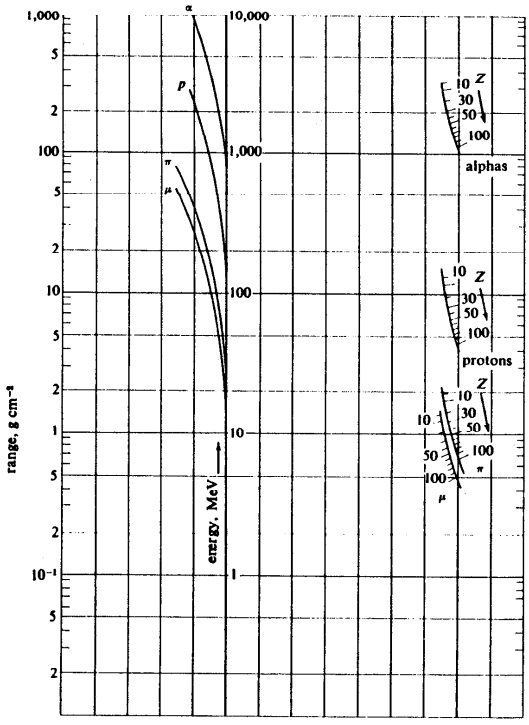

Figure 2-8 Nomogram by R. R. Wilson for range-energy relation. Left scales range in grams per square centimeter. Middle scale, kinetic energy in MeV. Right-hand scale, atomic number Z of stopping material and mass of particle. To use, connect range, energy, and Z by a straight line. [(3c 59).]

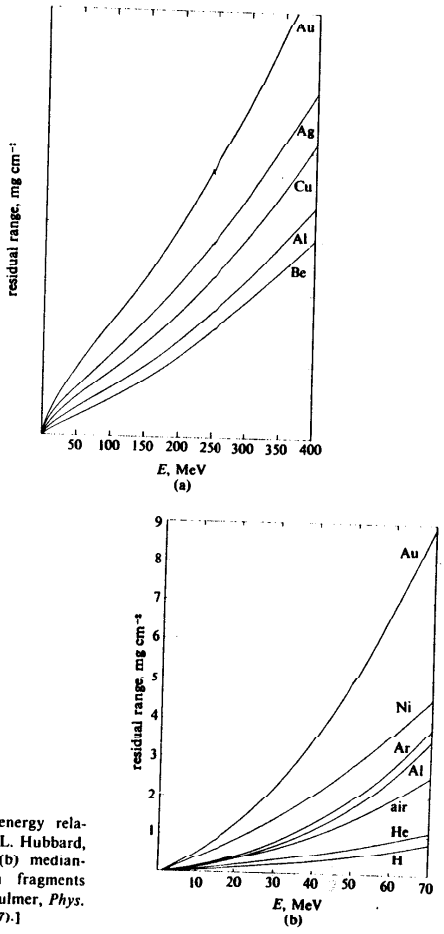

Figure 2-9 Range-energy relation for (a) Ar^{40} [E. L. Hubbard, UCRL 9053] and (b) median-mass heavy fission fragments ($A \simeq 140$). [C. B. Fulmer, *Phys. Rev.*, **108**, 1113 (1957).]

whereas the loss to electrons is proportional to

$$Z_1^2{}_{\text{eff}}\frac{Z_2}{m} \tag{2-3.17}$$

The first equation, (2-3.16), applies to close nuclear collisions where the entire charges of the fragment and the target are effective. In the case of electronic collisions only the net charge $Z_{1\text{eff}}$ of the fission fragment, with whatever electrons it carries along, is effective, and the target electrons have unit charge. The factor Z_2 of Eq. (2-3.17) arises from the presence of Z_2 electrons per nucleus. The approximate value of $Z_{1\text{eff}}$ is obtained by assuming that the fragment will lose all the electrons whose orbital velocity in the atom is smaller than the velocity of the fragment itself (see Fig. 2-9).

The two causes of energy loss considered above may be comparable, but the energy loss due to nuclear collisions is concentrated in few events, while the electronic collisions are much more uniformly distributed along the range. The nuclear collisions originate the peculiar branches observable in cloud-chamber pictures of fission fragments. The concentration of the nuclear energy loss in a few events is the cause of the great value of the straggling shown by fission fragments.

2-4 Energy Loss of Electrons

The energy loss of electrons is a much more complicated phenomenon than the energy loss by ionization of heavy ions, for in addition there is an energy loss due to electromagnetic radiation (*bremsstrahlung*) emitted in the violent accelerations that occur during collisions (Fig. 2-10). We shall consider the two effects separately, confining ourselves here to the energy loss due to ionization. The combination of radiation and ionization energy loss will be treated in Sec. 2-11. At low energies ($\ll 2mc^2$) the loss by ionization is much greater than that by radiation. For the derivation of the equations and a bibliography see the article of Bethe and Ashkin in (Se 59).

The energy loss by ionization may be treated in a manner similar to that used for heavy ions, but there are several important differences. It is necessary to take into account the identity of the particles involved in the collision and their reduced mass. The formula for nonrelativistic electrons is

$$-\frac{dE}{dx} = \frac{4\pi e^4 \mathcal{N}}{mv^2}\left(\log\frac{mv^2}{2I} - \tfrac{1}{4}\log 2 + \tfrac{1}{2}\right) \tag{2-4.1}$$

Except for small factors in the logarithmic term, this formula is the same as Eq. (2-3.11); hence, electrons and protons of the same nonrelativistic velocity will lose energy at the same rate. For high relativistic velocities the energy loss of electrons is

$$-\frac{dE}{dx} = \frac{4\pi e^4}{mc^2}\mathcal{N}\left[\log\frac{2mc^2}{I} - \tfrac{1}{3}\log(1-\beta^2)^{1/2} - \tfrac{1}{4}\log 8 + \tfrac{1}{16}\right] \tag{2-4.2}$$

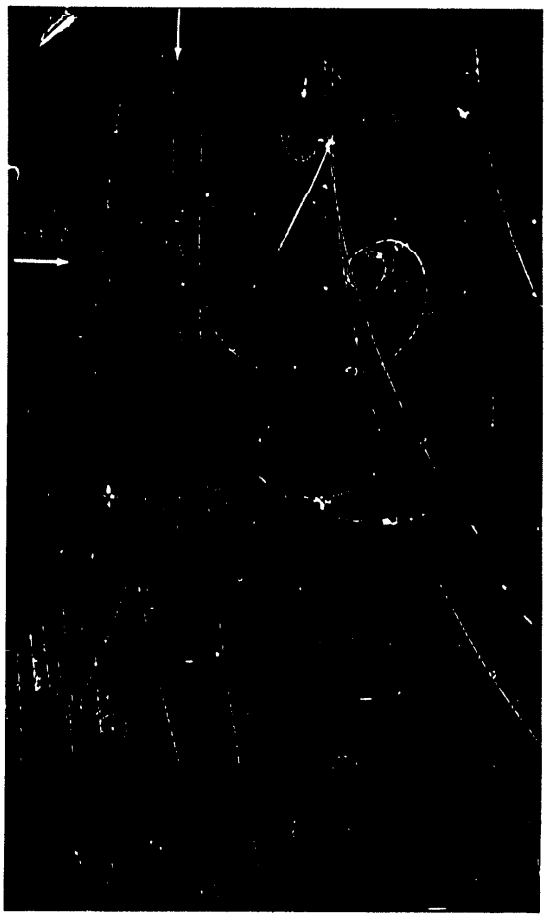

Figure 2-10 An electron loses energy by radiation as shown by the sudden increase in curvature of its trajectory. The emitted quantum makes an electron-positron pair. [Propane bubble chamber, courtesy Lawrence Radiation Laboratory.]

whereas for protons it is

$$-\frac{dE}{dx} = \frac{4\pi e^4}{mc^2}\mathcal{N}\left[\log\frac{2mc^2}{I} + 2\log\frac{1}{(1-\beta^2)^{1/2}} - 1\right] \quad (2\text{-}4.3)$$

At equal values of β, the two expressions differ by less than 10 per cent up to proton energies of 10^{10} eV. The difference between the average energy loss of electrons and positrons is even smaller.

An important practical difference between the behavior of heavy particles and electrons arises from the fact that the trajectories of electrons in matter are not straight lines, especially at low energies ($E \ll mc^2$). For this reason the actual path length of an electron passing through two points may be appreciably longer than the distance between these points measured on a straight line, as can be seen in Fig. 2-11. Thus, electrons of the same energy are not all stopped by the same thickness of material, and the concept of range has a limited validity.

For practical measurements of electron energy we can use the extrapolated range. It is important to note, however, that the geometry of the apparatus influences the result. Thus, in order to use the data found in the literature, one must reproduce the experimental arrangement used to obtain them (Fig. 2-12).

In the case of beta rays the electrons have a continuous energy spectrum, but it is still possible to find a relation between the upper limit of the energy of the spectrum E and the maximum range R (in g cm^{-2} of aluminum) of the electrons (Feather, 1938). A relation frequently used for a rapid determination of E (MeV) is

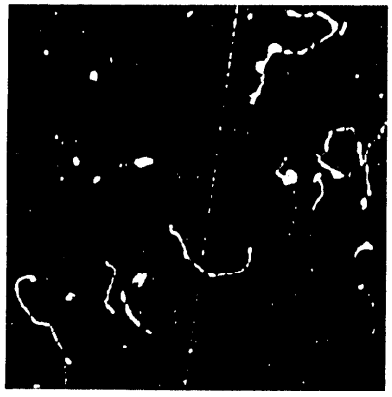

Figure 2-11 Slow electrons showing a curved path due to scattering. A fast electron goes straight. [Original from C. T. R. Wilson, 1923.]

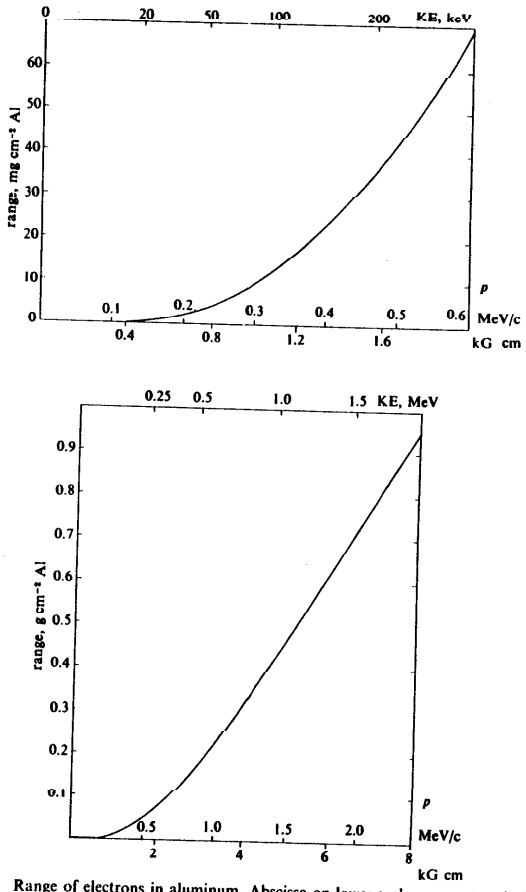

Figure 2-12 Range of electrons in aluminum. Abscissa on lower scale, momentum in MeV/c and in Br$=cp/e$ (3,327 G·cm $=$ 1 MeV/c). Abscissa on upper scale, KE in MeV. [(Se 59).]

$$R = \begin{cases} 0.542E - 0.133 & 0.8 < E < 3 \\ 0.407E^{1.38} & 0.15 < E < 0.8 \end{cases} \qquad (2\text{-}4.4)$$

See Fig. 2-13 for a range-energy plot usable for beta emitters.

2-5 Polarization Effects—Cerenkov Radiation

The derivation of Eq. (2-3.11) did not take into account the electrical polarization of the medium in which the heavy ion moves. The dielectric constant of the medium weakens the electric field acting at a distance from the ion, causing a decrease of the energy transfer to atoms located far from the ion, and hence a decrease in the mass stopping power. Thus, in the case of a medium in two phases of different density, such as water and vapor, the lower density phase has a higher mass stopping power. This effect is appreciable, however, only for relativistic velocities and seldom amounts to more than a few per cent.

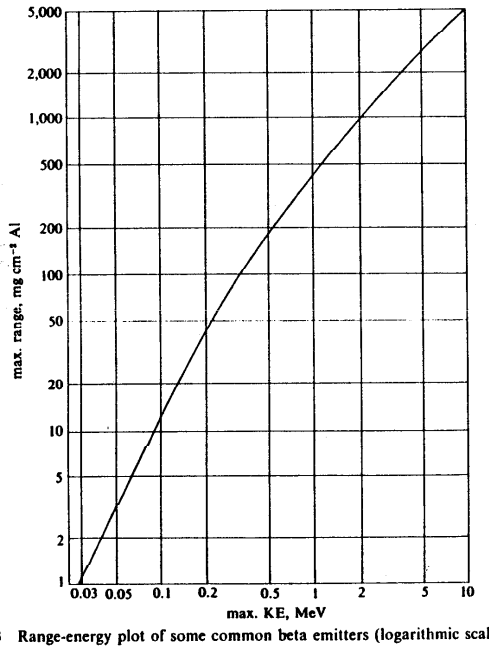

Figure 2-13 Range-energy plot of some common beta emitters (logarithmic scales). [(Si 55).]

Another important effect of the dielectric constant is the production of Cerenkov radiation (Cerenkov; Frank and Tamm, 1937). If a charge moves with a velocity βc in a medium of refractive index n, its electric field propagates with velocity c/n; and if $\beta c > c/n$, a phenomenon similar to the production of a bow wave results. Figure 2-14 gives the Huyghens' construction for the electromagnetic waves emitted by the particle along its path. At time $t = 0$, the particle is at O. One second later it is at P after traveling a distance $OP = \beta c$. The front of the electromagnetic wave is on the surface of the cone of aperture $\sin^{-1}(1/n\beta)$, which means that the rays of the corresponding light make an angle $\theta = \cos^{-1}(1/n\beta)$ with the trajectory of the particle. The intensity of the Cerenkov light can be calculated semiclassically [see for instance (Ja 62)]: for the number of quantum radiated per unit length with frequency between ν and $\nu + d\nu$ one has

$$dn = \frac{2\pi e^2}{\hbar c}\left(1 - \frac{1}{n^2\beta^2}\right)\frac{d\nu}{c} = \frac{2\pi e^2}{\hbar c}\sin^2\theta\,\frac{d\nu}{c} \qquad (2\text{-}5.1)$$

In the spectral region between 3,000 and 6,000 Å Eq. (2-5.1) thus gives approximately $750 \sin^2\theta$ photons per centimeter. The spectrum is a continuum.

The light is polarized, with its electric vector pointing in the PQ direction. The measure of the angle θ of Cerenkov light may be used to determine the value of β for the particle. The density effect and the Cerenkov light are interrelated, both being functions of the dielectric constant of the medium.

2-6 Ionization in Gases and Semiconductors

A charged particle passing through a gas ionizes it. However, only part of the energy goes into ionizing the gas and into imparting kinetic energy to the electrons. A sizable fraction is spent in exciting the atoms below the ionization limit, and some of it is then transformed into detectable scintillation light. The average amount of energy required per ion formed, is remarkably independent of the charge, mass, and velocity of the particle producing the ionization, but depends on the gas in which the ions are formed. There is no simple physical explanation

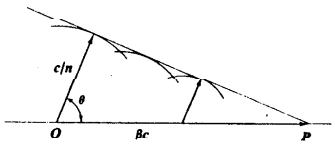

Figure 2-14 Huyghens' construction for electromagnetic waves emitted by a moving charged particle. Origin of Cerenkov radiation.